SAND2015-8357R

Thermal Mechanical Stress Modeling of GCtM Seals

Steve Dai and Robert Chambers
Sandia National Laboratories
Albuquerque, NM 87185

Abstract

Finite-element thermal stress modeling at the glass-ceramic to metal (GCtM) interface was conducted assuming heterogeneous glass-ceramic microstructure. The glass-ceramics were treated as composites consisting of high expansion silica crystalline phases dispersed in a uniform residual glass. Interfacial stresses were examined for two types of glass-ceramics. One was designated as SL16 glass-ceramic, owing to its step-like thermal strain curve with an overall coefficient of thermal expansion (CTE) at 16 ppm/°C. Clustered Cristobalite is the dominant silica phase in SL16 glass-ceramic. The other, designated as NL16 glass-ceramic, exhibited clusters of mixed Cristobalite and Quartz and showed a near-linear thermal strain curve with a same CTE value.

Induced by the α-β inversion in Cristobalite crystals, the concentrated tensile stress generated from a Cristobalite cluster in SL16 glass-ceramic caused localized separation at the GC-M interface. For NL16 glass-ceramic the tensile stress associated to the clusters with mixed Cristobalite and Quartz reduced significantly, resulting improved sealing at the GC-M interface.

The improved strain linearity of NL16 glass-ceramics was attributed to two factors: 1) the far apart α-β inversion temperatures of Cristobalite and Quartz that distribute the inversion induced volume changes over a wide temperature range, and 2) the reduced weight percentages of the two crystalline phases in NL16 led to much smaller inversion induced volume changes, versus a single large volume change caused by Cristobalite in SL16 glass-ceramic.

Introduction

In all previous Sandia modeling efforts on GCtM sealed components the glass-ceramic was treated as a homogeneous material like the glass in Glass-to-Metal (GtM) seals. Increasingly the assumption seemed not to adequately capture the true localized effects resulting from a heterogeneous glass-ceramic microstructure.

Figs. 1a and 1b are SEM images of longitudinal and transverse cross sections of the GC-M interfaces of ISL headers. At low magnification (Figs. 1a and 1b) there is hardly noticeable separation betweenglass-ceramic and metal. Close inspection of the GC-M interface, however, does reveal localized separation at the interface, as marked by the red arrows in the high magnification SEM images in Figs 1c and 1d. The distribution of the gaps appeared to be random, not necessarily tied to specificpositions at the interface, for example air-GC-M triple joint. The hermeticity of the GCtM seals depends largely on the connectivity among the localized separations: the seal may remain hermetic despite the existence of isolated separations, but could fail when a leak path forms through the linkage of the interfacial gaps.

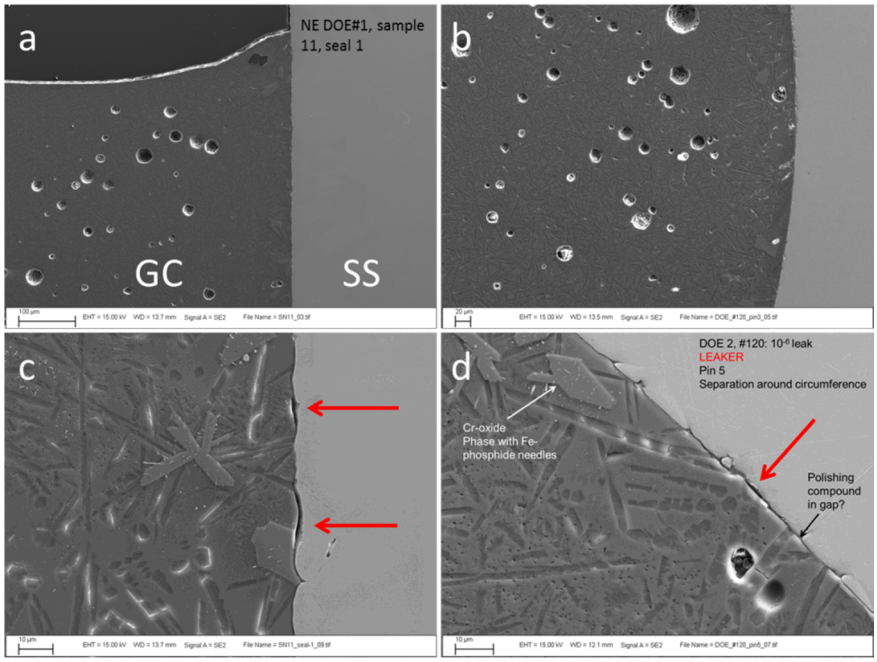

Figure 1. SEM images of GCtM seals. (a) and (b) are the low magnification longitudinal (cut parallel to pin) and transverse (cut perpendicular to pin) cross sections. (c) and(d) are correspondent high magnification images where the localized separation between GC and SS are highlighted by red arrows.

Fig. 2 is a colorized SEM image of glass-ceramic at CTE=17 ppm/°C showing various phases (Rodelas, Buchheit, & Tandon, 2007). The most predominant crystalline phase is the elongated Li_2SiO_3. In between the long Li_2SiO_3 crystals there are **clusters** of seemly equiaxed Cristobalite crystals at a size of a few

micrometers. The clusters reach 10s μm in size. All crystals are seen embedded in an inter-connected residual glass. Micro cracks, cutting across both crystalline phases and residual glass, indicate existence of localized stresses. The image reveals the heterogeneity of microstructure of glass-ceramics and strongly suggests the necessity of modeling it as a composite material.

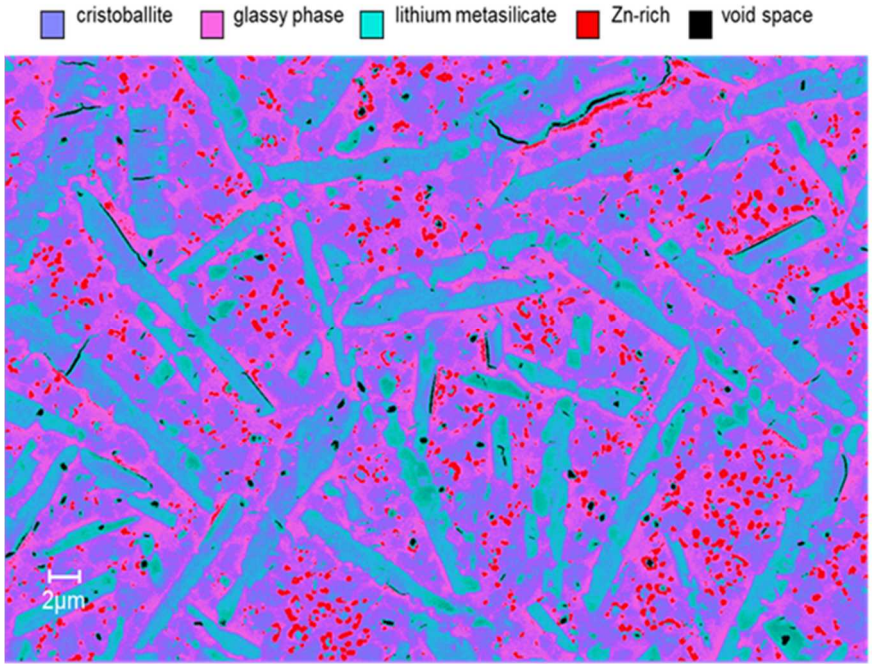

Figure 2. SEM image of the composite structure of GC at CTE 17.

Two glass-ceramics with approximately same CTE value at 16 ppm/°C, SL16 and NL16, were processed using the thermal schedules in Figs. 3a and 3b. The monotonic cooling from peak sealing temperature in Fig. 3a crystallizes predominantly Cristobalite. The low-high 2 step-hold temperatures in Fig. 3b allowed formation of Quartz in 1st hold and subsequent heating to 2nd hold temperature, and crystallization of Cristobalite at the 2nd higher hold temperature.

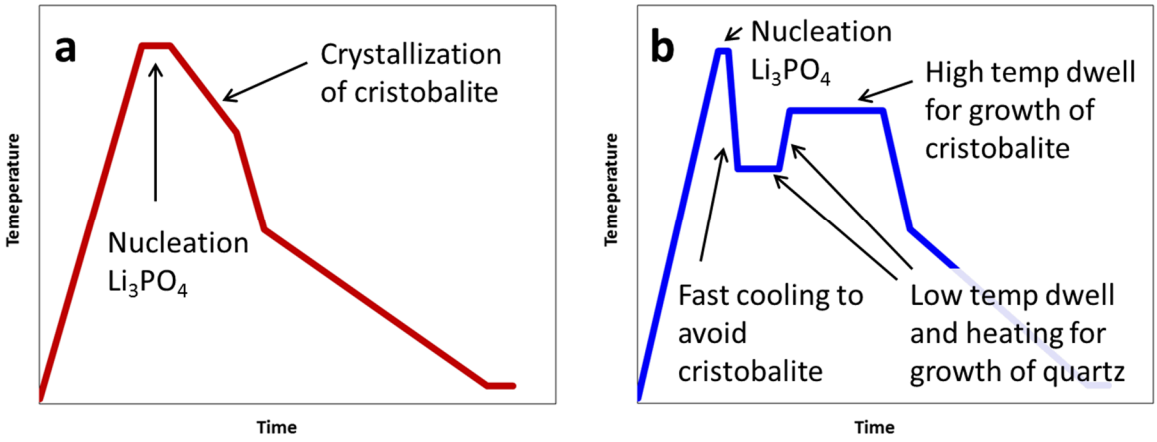

Figure 3. Sealing profile for growth of (a) cristobalite, and (b) both quartz and cristobalite.

Fig. 4 shows XRD patterns of SL16 and NL16 glass-ceramics. The Li_2SiO_3 and Li_3PO_4 crystalline phases exist in both glass-ceramics. The SL16 has a dominant Cristobalite peak with a presence of small amount of Quartz. On the other hand, the NL16 shows a reduced cristobalite peak with a much enhanced peak of Quartz. The XRD study provides direct and unambiguous evidence of the growth of Quartz followed by Cristobalite using the new sealing profile (Fig. 3b).

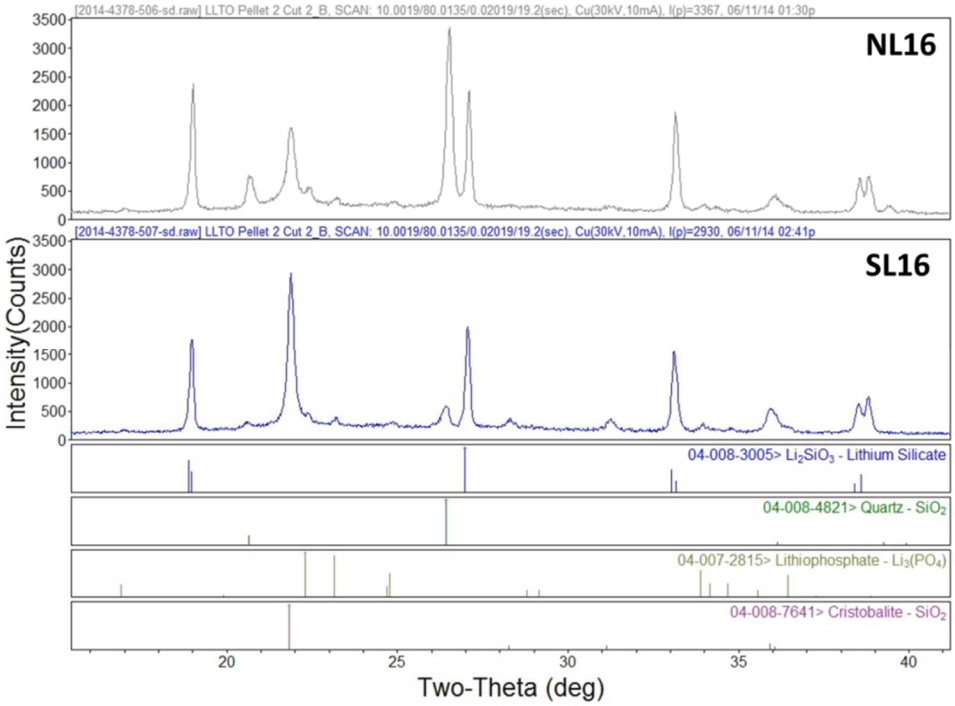

Figure 1. XRD patterns of SL16 and NL16 glass-ceramics.

Table 1 shows the weight percentage of crystalline and amorphous phases in SL16 and NL16 glass-ceramics. Data reveal considerable differences between the two in terms of Cristobalite, Quartz, and amorphous phase fractions. At 24.4 wt% the Cristobalite is the dominant SiO_2 phase in SL16 glass-ceramic in which the low quartz is at a minor 2.5 wt%. For NL16 glass-ceramic the Cristobalite decrease to 16.6 wt% while the low Quartz increases to 13.7 wt%. The weight fractions of the Li_2SiO_3 and Li_3PO_4 phases appear to remain similar in the two glass-ceramics.

Table 1. Quantitative analysis of phases in SL16 and NL16 glass-ceramics.

Phase	SL16		NL16	
	wt%	±wt%	wt%	±wt%
Quartz Low SiO_2	2.51	0.081	13.71	0.190
Cristobalite SiO_2	24.37	0.325	16.55	0.257
Li_2SiO_3	36.82	0.480	37.95	0.422
Li_3PO_4	7.94	0.467	7.36	0.434
Amorphous	28.36	0.586	24.42	0.581

Fig. 5 shows thermal strains of 304L stainless steel shell, Paliney-7 pin and SL16 and NL16 glass-ceramics. Comparing to SL16 glass-ceramic which shows a step change in thermal strain at 220°C, the NL16 GC shows a much reduced step at the same temperature plus a diffused second step around 470°C. The second broad step in NL16 is believed to be induced by the α-β phase transition in Quartz. The linear aggression R^2 data in the insert quantify the much improved linearity of NL16 over the SL16 glass-ceramic.

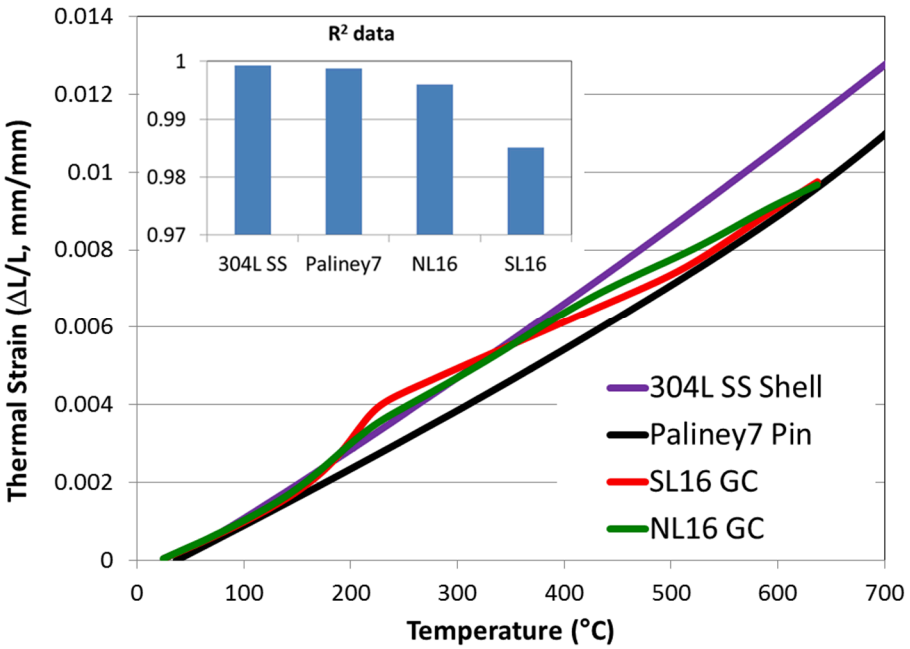

Figure 5. Thermal strain curves of 304L SS shell, Paliney-7 pin and SL16 and NL16 GCs. The insert shows the corresponding R2 data.

Approach

Thermals strains of Cristobalite and Quartz are shown in Fig. 6(Bauleke, 1978). Clearly large volume changes associated with the α-β inversions exist in both crystals. The inversion temperature is ~ 220 °C for Cristobalite and 573 °C for Quartz.

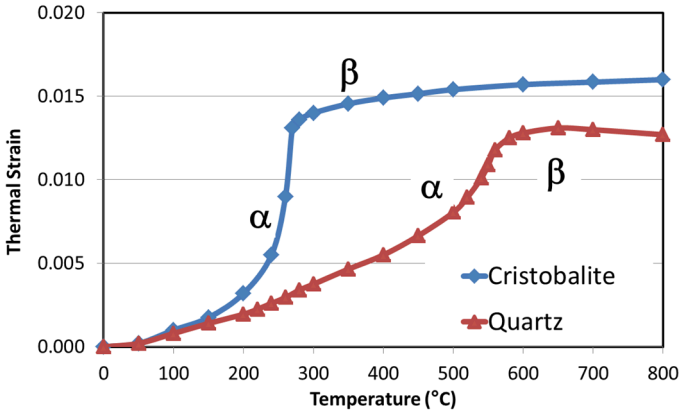

Figure 6. Thermal strains of Cristobalite and Quartz crystals showing α-β inversions.

Model of SL16 glass-ceramic

The model assumes a cluster of 5x5 Cristobalite slanted discs at 5 μm diameter dispersed in a uniform residual glass. The SL16 glass-ceramic fills in a 304L stainless steel ring without a center pin. Assuming axial symmetry a 5° thin slice was set as a unit where the Cristobalite cluster is sandwiched between two 1° slices of glass. Details of the model are shown in Fig. 7.

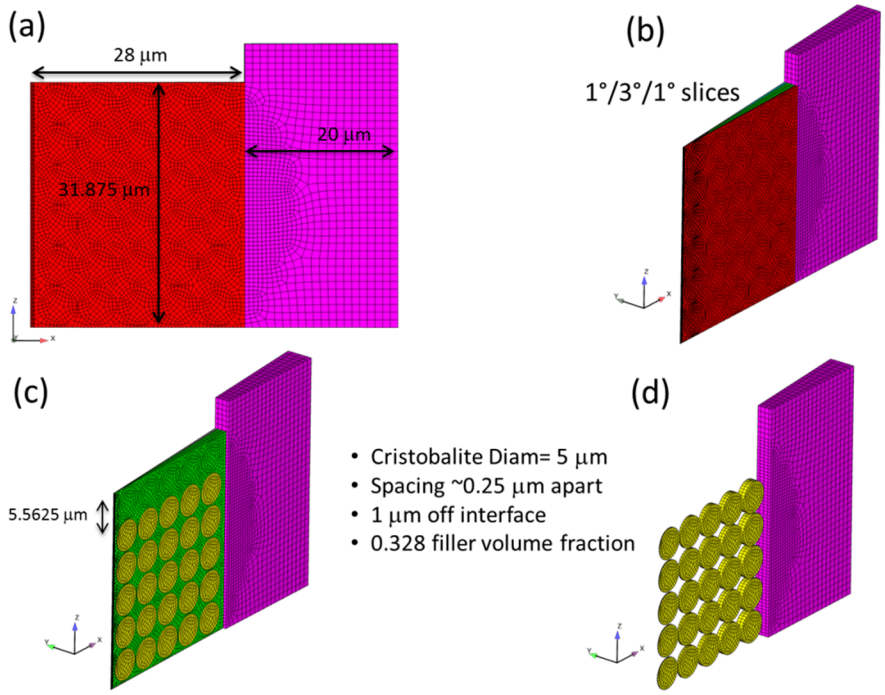

Figure 7. Model for SL16 glass-ceramic.

Fig. 7 shows the thermal strain curve of stainless steel, Cristobalite andassumed homogeneous residual glass. The stress free temperature from cooling was set at 500°C.

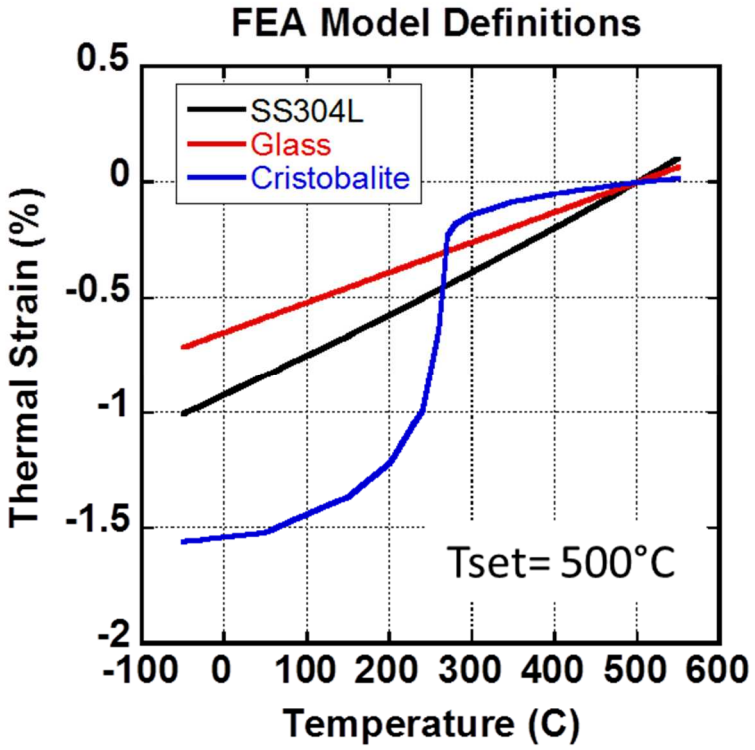

Figure 6. Thermal strains for SL16 glass ceramic model.

Table 2 lists Young's modulus and Poisson's ratios of the three materials.

Table 2. Mechanical properties of materials (Pabst & Gregorova, 2013).

Property	304L Stainless Steel	Residual Glass	Cristobalite	Quartz
Young's Modulus (E, GPa)	193	90	62	95
Poisson's Ratio (v)	0.27	0.165	0.169	0.108

Model of NL16 glass-ceramic

For NL16 glass-ceramic the cluster is composed of mixed Cristobalite and Quartzdiscs. Table 3 shows that the volume ratio of Cristobalite to Quartz is about 3 to 2 based on wt% data in Table 1.

Table 3. Volume percent of Cristobalite and Quartz in SL16 and NL16 glass-ceramics.

Phase	**NL16 GC**	
	wt%	Appx vol%
Quartz (2.65 g/cc)	13.71	12
Cristobalite (2.34g/cc)	16.55	18

The mixture of Cristobalite and Quartz was modeled in three configurations as shown in Fig. 7 where C stands for Cristobalite and Q for Quartz, 1) the particles are aligned in radial direction, 2) alignedin longitudinal Z direction, and 3) random mixture.

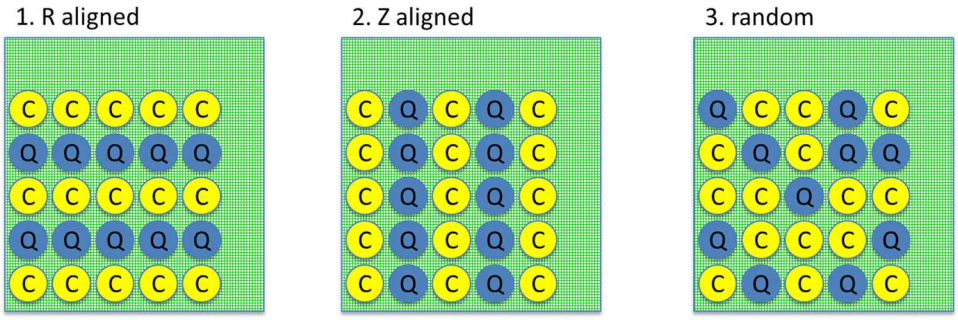

Figure 7. Configurations of mixed Cristobalite and Quartz cluster.

Results and Impacts

SL16 glass-ceramic

Cooling from 500 °C to 20 °C, Fig.8 shows both the slip along and the separation at the GCtM interface. Considering that the CTE of SL16 glass-ceramic is lower than that of 304L steel, which suggests an overall compression on glass-ceramic by the steel, the separation at the interface clearly demonstrates the effect of α-β inversion in the clustered Cristobalite phase. It is important to note that the gap is localized, occurring only at the interface next to a Cristobalite cluster.

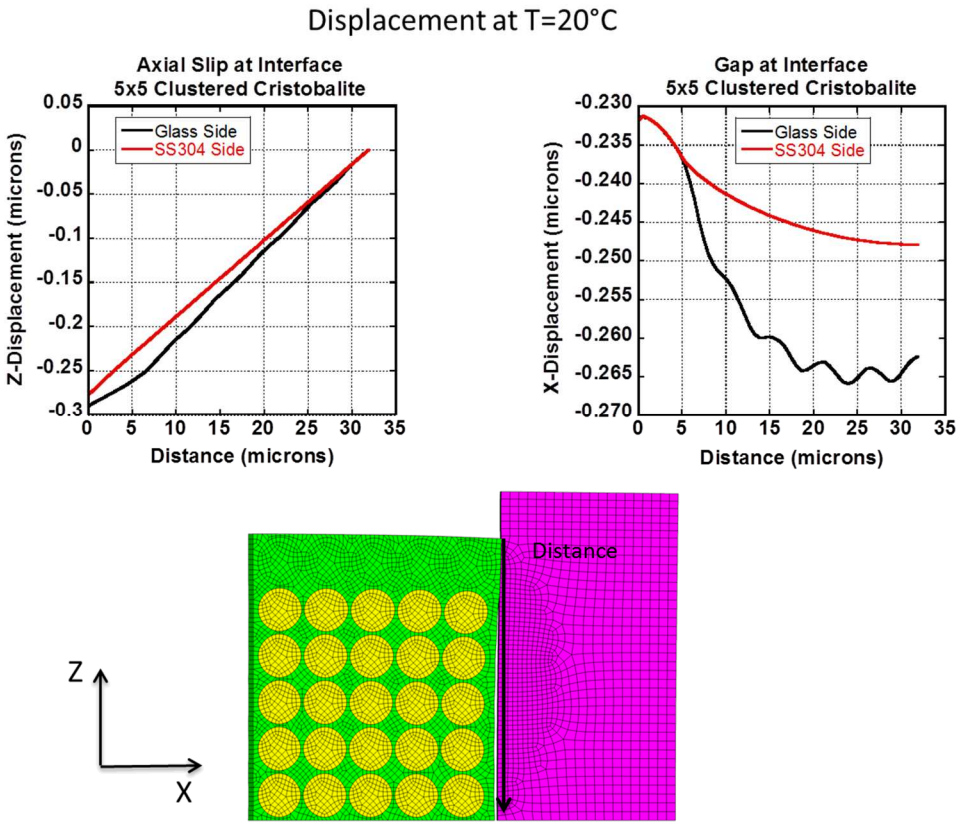

Figure 8. Axial slip (along Z) and gap (along X) at the GC-M interface.

Impact: this is first attempt in Sandia to model the stresses in GCtM seals treating the glass-ceramic as a composite material. Qualitatively the model confirmed localized separations at the GCtM interface. The result is consistent with the actual gaps seen in SEM cross section images of GC-M seals.

NL16 glass-ceramic

The stresses were analyzed in three different mixing configurationsin Fig. 7.

Case 1: R aligned. Fig. 9 shows the slip along and the separation at the interface. The slip nearly disappears. Small gaps correlating to the Cristobalite rows still exist. However the glass-ceramic seals to metal where the Quartz rows exist. Overall the NL16 demonstrated much improved seals tometal.

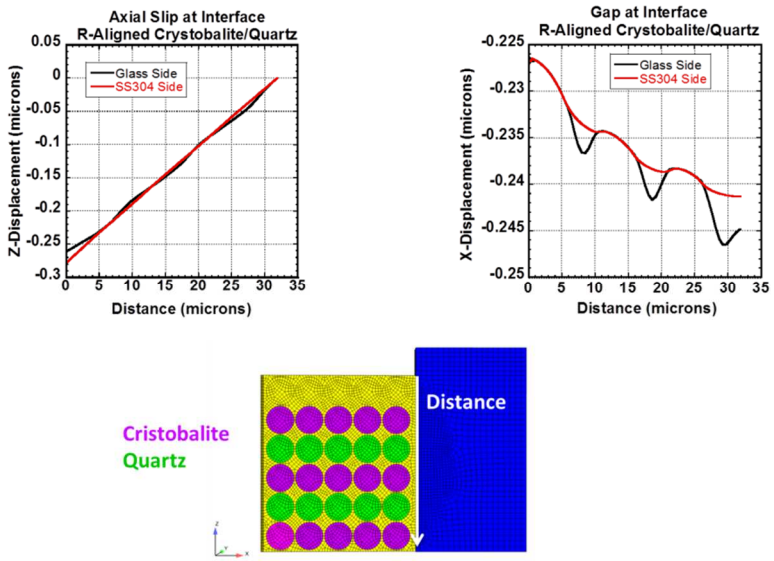

Figure 9. Axial slip and gap at the GC-M interface assuming Cristobalite and Quartz are aligned along the radial direction.

Case 2: Z aligned. Fig. 10 shows the slip along and the separation at the interface. Similarly the slip nearly disappears. There are only small periodic gaps mirroring the position ofCristobalite discs in the cluster. This seal is much improved over the SL16 glass-ceramic.

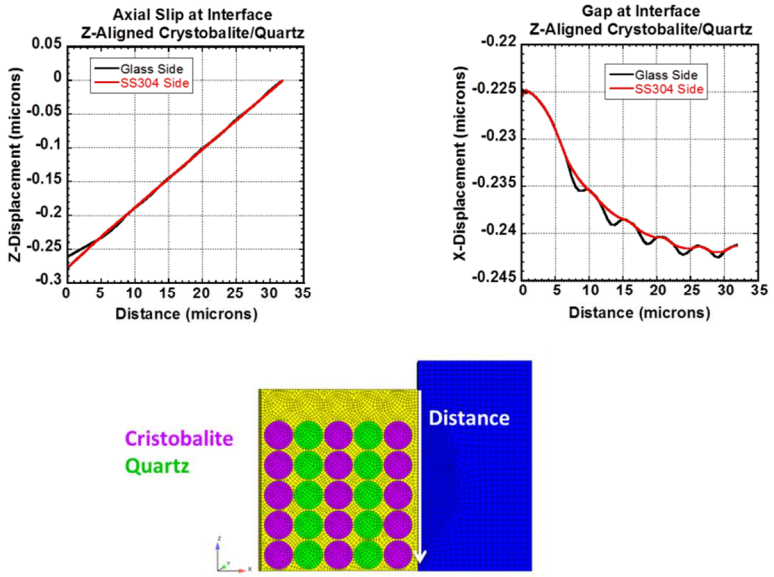

Figure 10. Axial slip and gap at the GC-M interface assuming Cristobalite and Quartz are aligned along the axial (Z) direction

Case 2: Z aligned. Fig. 11 shows the slip along and the separation at the interface. Again the slip nearly disappears. There are only small gaps mirroring the position of Cristobalitediscs in the cluster. This seal is also much improved over the SL16 glass-ceramic.

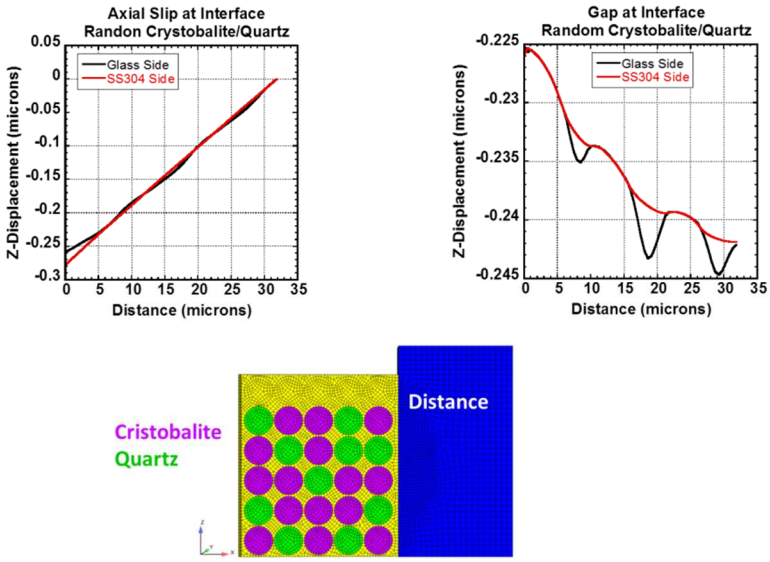

Figure 11. Slip along and the gap at GC-M interface with random Cristobalite and Quartz distribution.

Impact: the model suggests that NL16 glass-ceramic with mixed Cristobalite and Quartz phases could significantly improve the GC-M seals.

Conclusions and Future Work

Models treating glass-ceramics as a composite were established to analyze thermal mechanical stresses in GCtM seals. Localized separation at the GCtM interface wasconfirmed for SL16 glass-ceramic where the α-β inversion causes the clustered Cristobalite moving away from the steel. For NL16 glass-ceramic the seal improves significantly due to the co-existence of Cristobalite and Quartz.

Future work will include irregularities at the GCtM interface to examine whether the GC can re-seal to the steel upon interfacial slipping and separation.

Summary of Findings and Capabilities Related to Aging

- FE model treating glass-ceramics as composite was established
- Model confirmed localized separation at the GC-M interface as observed in SME cross section analysis on seals using SL16 glass-ceramic
- Model predicted NL16 glass-ceramic would improve the seals, and enhance the long term reliability of the GCtM seals
- The simulation will directly impact several GCtM sealed components and define paths to for reduced aging and improved long term reliability

References

Bauleke, M. P. (1978). How to Solve the Problems of Body Cracking and Glaze Popping in Stoneware Bodies. *Kansas Geological Survey, 211*(4), 23-27.

Dai, S. (2015). *Glass-ceramic to Stainlless Steel Bonding.* SAND2015-0180. Albuquerque, New Mexico: Sandia National Laboratories.

Pabst, W., & Gregorova, E. (2013). ELASTIC PROPERTIES OF SILICA POLYMORPHS – A REVIEW. *Ceramics, 57*(3), 167-184.

Rodelas, J. M., Buchheit, T., & Tandon, R. (2007). *Characterization of Glass-Ceramic to Metal Interfaces via Nano Indentation.* Sandia National Laboratories, Albuquerque.

Administrative Addendum

Steve Dai, 1800 Materials Science Seminar, "Glass-ceramic to metal seals", Apr 2015

Milestone Status:

Deliverable	Date	Status
1. Models on thermal mechanical stress analysis with step-like and near-linear thermal strains of GC, and model validation	6/30/2015	Completed
2. Experimental validation	9/30/2015	Extended to FY16

Sandia National Laboratories is a multi-program laboratory managed and operated by Sandia Corporation, a wholly owned subsidiary of Lockheed Martin Corporation, for the U.S. Department of Energy's National Nuclear Security Administration under contract DE-AC04-94AL85000.